PCCP

PAPER

View Article Online
View Journal | View Issue

Cite this: *Phys. Chem. Chem. Phys.*, 2020, **22**, 7935

Hydrogen diffusion out of ruthenium—an *ab initio* study of the role of adsorbates

Chidozie Onwudinanti,[ab] Geert Brocks,[bc] Vianney Koelman,[ab] Thomas Morgan[a] and Shuxia Tao *[b]

Received 27th January 2020,
Accepted 17th March 2020

DOI: 10.1039/d0cp00448k

rsc.li/pccp

Hydrogen permeation into mirrors used in extreme ultraviolet lithography results in the formation of blisters, which are detrimental to reflectivity. An understanding of the mechanism via which hydrogen ends up at the interface between the top ruthenium layer and the underlying bilayers is necessary to mitigate the blistering damage. In this study, we use density functional theory to examine the ways in which hydrogen, having entered the near-surface interstitial voids, can migrate further into the metal or to its surface. We show that with hydrogen and tin adsorbed on the ruthenium surface, diffusion to the surface is blocked for interstitial hydrogen in the metal, making diffusion further into the metal more likely than out-diffusion. The dependence on surface conditions matches and confirms similar findings on hydrogen permeation into metals. This suggests control and modification of surface conditions as a way to influence hydrogen retention and blistering.

1 Introduction

There are several things that can happen when a metal is exposed to hydrogen. A certain amount of the gas will usually adsorb on the metal surface, some may end up absorbed into the interstitial sites in the metal's crystal lattice, and in some cases the metal bonds with the hydrogen to form metal hydrides. The extent to which each of these possibilities occurs depends on the metal involved, and the amount and state of the hydrogen supplied to it. This metal-hydrogen interaction is of great importance for a number of technological systems, spanning a wide range from heterogeneous catalysis[1] to separation,[2,3] storage,[4] and sensors.[5] Hydrogen plasma and metals also come in contact in nuclear fusion experiments and reactors.[6]

The interaction of hydrogen and ruthenium has been studied extensively, particularly in the field of catalysis. In an altogether different technological application, the metal has found use as a capping layer on the multi-layer mirrors (MLMs) used in extreme ultraviolet (EUV) lithography.[7,8] The MLM consists of 40–60 molybdenum/silicon bilayers, each about 6 to 7 nanometres thick, and is capped by a ruthenium layer. Tin plasma is the source of EUV photons for the lithographic system, and tin debris can be deposited on the mirror. Hydrogen is used as a buffer for the optics, and to etch away contaminants. It comes into contact with the metal, and may penetrate the surface. It can then diffuse through the bulk to the interface(s) of the multi-layer structure, where it recombines to form pockets of H_2 gas. When these pockets reach a critical pressure, the layers separate, resulting in blistering of the mirror and loss of reflectivity.[9,10] This process appears to be facilitated by tin.

Ruthenium ought to be an ideal capping material, protecting the MLM against hydrogen. In addition to its suitable mechanical and optical properties, it also exhibits low H solubility.[11] Although H_2 dissociates and asdsorbs on the surface,[12] the resulting atoms do not penetrate the Ru lattice easily. In a previous publication,[13] we reported that the energy of formation of interstitial hydrogen in ruthenium was found to be positive for both interstitial sites. Our calculations showed that the DFT-calculated energy barrier to subsurface penetration is large for hydrogen, but the presence of tin on the surface leads to a significant lowering of the barrier. These results, and the observed blistering after tin contamination, led to the question: since hydrogen exhibits low solubility in ruthenium, why does the hydrogen injected by tin (hydrides) remain in the ruthenium, and subsequently form blisters at the interface(s)?

We posit that the coverage of the ruthenium surface by adsorbates obstructs the exit of hydrogen from the near-surface region to the surface and the gas phase, thus playing an important role in the blistering process. A number of phenomena have their basis in such restriction of access to the surface. Livshits *et al.*[14] linked superpermeability of a metal membrane to the presence of chemically active adlayers on the upstream surface.

[a] *DIFFER–Dutch Institute for Fundamental Energy Research, Eindhoven, The Netherlands*
[b] *Center for Computational Energy Research, Department of Applied Physics, Eindhoven University of Technology, Eindhoven, The Netherlands. E-mail: s.x.tao@tue.nl*
[c] *Computational Materials Science, Faculty of Science and Technology and MESA+ Institute for Nanotechnology, University of Twente, 7500 AE Enschede, The Netherlands*

Carbon impurities in a hydrogen plasma were found to increase blistering in tungsten targets.[15] A palladium–gold alloy was shown to accumulate hydrogen in the near-surface region when the hydrogen exit path was affected by adsorbed CO.[16] This effect also occurs without impurities; Soroka *et al.*[17] proposed that the saturation of a ruthenium thin-film surface with hydrogen inhibits hydrogen removal from the underlying yttrium hydride layer. In all these cases, the exit of hydrogen from the bulk metal is impeded by conditions on the surface which cause reduced bulk-to-surface diffusion, recombination, and desorption.

In this article, we examine the different paths and mechanisms through which hydrogen, having reached the interstitial sites in the metal, eventually leaves the bulk and ends up either in the gas phase above the ruthenium capping layer or in the pockets of molecular hydrogen which form the blisters. We show that the availability of sites on the metal surface plays a key role in the out-diffusion of hydrogen. Thus, saturation of the surface with adsorbed hydrogen hinders the removal of hydrogen from the bulk. Our calculations therefore indicate that near-complete coverage of the ruthenium surface will result in more hydrogen reaching the interface between the thin ruthenium layer and its substrate, where it can form blisters.

2 Computational details

The results presented in this work are based on computations performed within the framework of Density Functional Theory (DFT), as implemented in the Vienna Ab Initio Simulation Package (VASP).[18–20] The calculations were performed with the generalized gradient approach as proposed by Perdew, Burke, and Ernzerhof (PBE),[21] with the following key convergence parameters: a kinetic energy cutoff of 400 eV, a residual force criterion of 1×10^{-2} eV Å^{-1}, and a 1×10^{-5} eV energy convergence criterion. Slab calculations were performed with a $(9 \times 9 \times 1)$ Γ-centred k-points grid, while bulk calculations were done with a $(9 \times 9 \times 9)$ grid; all atoms were allowed to relax in the optimization process. Transition state calculations were carried out using the Climbing Image Nudged Elastic Band (CINEB) algorithm,[22] with a force criterion of 1×10^{-2} eV Å^{-1} and one (1) to five (5) intermediate geometries for the transition state search.

The calculated lattice parameters for hexagonal close-packed (hcp) ruthenium are $a = 2.69$ Å and $c/a = 1.58$, which are in good agreement with experimental results, 2.71 Å and 1.58, respectively.[23] The Ru(0001) surface is modelled as a slab of seven layers using a (2×2) cell, with $\sim$ 15 Å of vacuum between the periodic images in the z-direction. The number of layers and the vacuum height were found to give accurate results at reasonable computational cost—the calculated surface energy changes by less than 2% from 7 layers to 11 layers.

For hydrogen, the energy of adsorption is computed per the definition

$$E_{\mathrm{ads}} = \frac{1}{n}\left(E_{\mathrm{nH,surf}} - E_{\mathrm{surf}} - \frac{n}{2}E_{\mathrm{H_2}}\right), \quad (1)$$

where $E_{\mathrm{nH,surf}}$, E_{surf}, and $E_{\mathrm{H_2}}$ stand respectively for the energy of the ruthenium slab with n adsorbed hydrogen atoms, the energy of the clean ruthenium slab, and the energy of the hydrogen molecule. The formation energy of interstitial hydrogen, normalised to the hydrogen concentration, is calculated according to the definition

$$\Delta E_{\mathrm{H_2}} = \left(E_{\mathrm{M}_x\mathrm{H}_y} - xE_{\mathrm{M}} - \frac{y}{2}E_{\mathrm{H_2}}\right)\Big/\frac{y}{2}, \quad (2)$$

where x, y are respectively the number of metal atoms and the number of hydrogen atoms, while $E_{\mathrm{M}_x\mathrm{H}_y}$, E_{M}, and $E_{\mathrm{H_2}}$ stand respectively for the total energy of the metal hydride, the energy of each bulk metal atom, and the energy of a hydrogen molecule.

Due to the low mass of the hydrogen atom, its adsorption and diffusion are, in general, influenced by zero-point energy (ZPE). The ZPE is calculated by the relation

$$\mathrm{ZPE} = \frac{\sum_i h\nu_i}{2}, \quad (3)$$

where ν_i is a real normal mode frequency. The zero point energy for a hydrogen molecule (H_2) calculated thus is 0.27 eV (0.135 eV per H atom), corresponding to a vibrational mode of 4354 cm^{-1}, in good agreement with the experimentally-determined value of 4401 cm^{-1}.[24] We have computed the ZPE for a hydrogen atom on the surface and in the interstitial sites, as well the transition states. The energy barriers reported in the subsequent chapters include ZPE corrections, which are also taken into account in the calculation of diffusion coefficients.

Diffusion coefficients are commonly expressed in the general form,

$$D = D_0 e^{\frac{-Q}{k_B T}}, \quad (4)$$

where D_0 is a prefactor, Q is the activation energy, k_B is the Boltzmann constant, and T is the temperature. According to the approach proposed by Ishioka and Koiwa,[25] two diffusion coefficients, $D_\perp$ and $D_\parallel$, can be computed for interstitials with multiple jump frequencies in an hcp lattice with parameters a and c. These diffusion coefficients correspond to diffusion perpendicular to the c axis and parallel to it. The diffusion coefficients are obtained *via* the following formulae:

$$D_\perp = \frac{\omega_{\mathrm{TO}}\omega_{\mathrm{OT}}}{\omega_{\mathrm{TO}} + 2\omega_{\mathrm{OT}}}a^2 \quad (5)$$

$$D_\parallel = \frac{\omega_{\mathrm{TO}}(3\omega_{\mathrm{OO}}\omega_{\mathrm{TO}} + 2\omega_{\mathrm{OO}}\omega_{\mathrm{TT}} + 3\omega_{\mathrm{TT}}\omega_{\mathrm{OT}})}{4(2\omega_{\mathrm{TT}} + 3\omega_{\mathrm{TO}})(\omega_{\mathrm{TO}} + 2\omega_{\mathrm{OT}})}c^2 \quad (6)$$

where a, c are the lattice parameters, and $\omega_{xx} = \nu_{ij}e^{\frac{-E_b}{k_B T}}$ is the jump rate from one site to another, derived from ν_{ij}, the effective frequency;[26] E_b, the energy barrier; k_B, the Boltzmann constant; and T, the temperature. A linear fit of the diffusion coefficient curves against temperature gives the diffusion coefficient pre-factors ($D_{0\perp}$ and $D_{0\parallel}$) and activation energies ($Q_\perp$ and $Q_\parallel$) according to the Arrhenius plot of eqn (4).

3 Results

Hydrogen on the surface

Exposure of ruthenium to hydrogen will result in adsorption of hydrogen on the metal, and our study starts with a consideration of adsorption. We choose to study the 0001 surface of ruthenium for two related reasons: first, this plane has the lowest surface energy, and will therefore dominate the exposed surface of a thin film; second, this surface is widely studied and represented in the literature, which allows a measure of validation of the computed energies and geometries.

The Ru(0001) surface offers a number of adsorption sites. Two of these sites, labelled fcc and hcp sites, allow three-fold coordination of H with surface Ru atoms, and have the most negative adsorption energies (see Fig. 1). Indeed, all sites show negative adsorption energies, with the top site least favourable. The values remain negative at 100% coverage, *i.e.* up to 1 H atom per surface Ru atom, with all fcc sites occupied. Previously-published first-principles calculations[27,28] show a similar trend in energies of adsorption, with the slight variations in absolute values explained by differences in parameters and software used for the DFT calculations. We thus confirm that hydrogen adsorption on the ruthenium surface is favourable, and that exposing ruthenium to hydrogen will result in saturation of the surface by dissociated hydrogen atoms.

Hydrogen in the bulk

Hydrogen in ruthenium is found as discrete atoms located in the interstices of the hexagonal close-packed lattice. An interstitial atom can occupy one of two sites, octahedral or tetrahedral, relative to the surrounding nearest neighbour metal atoms.

In the close-packed lattice, the octahedral sites, which are formed by 6 atoms at the vertices, are larger than the tetrahedral voids, formed by 4. The calculated formation energy of the interstitial hydride, shown at 154 concentration (H/Ru) in Fig. 2, indicates that the octahedral site is preferable. Its 0.34 eV formation energy is much lower than the 0.84 eV of the tetrahedral site. For the subsurface octahedral site which we focus on subsequently, the energy value is nearly the same, 0.30 eV at 128 concentration; this is calculated for a slab, as opposed to the preceding bulk values. Nonetheless, we can conclude that the subsurface state is very similar to the bulk interstitial state.

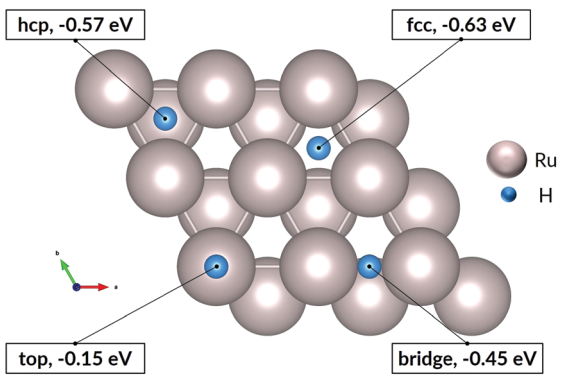

Fig. 1 Adsorption sites for H on the Ru(0001) surface, with corresponding energies of adsorption.

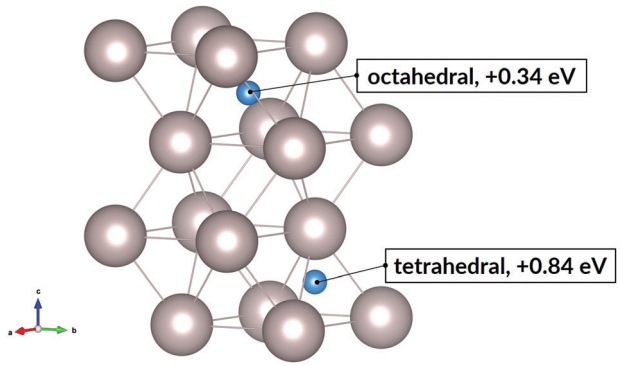

Fig. 2 Interstitial sites and the corresponding hydride formation energies at hydrogen concentration (H/Ru) equal to 154.

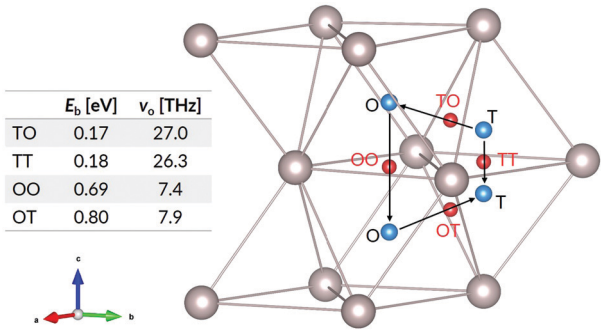

	E_b [eV]	ν_o [THz]
TO	0.17	27.0
TT	0.18	26.3
OO	0.69	7.4
OT	0.80	7.9

Fig. 3 Jump paths, ZPE-corrected energy barriers, and effective frequencies for H in Ru. The blue spheres show the interstitial sites and the red spheres show transition states between the sites.

In general, the endothermic nature of interstitial hydride formation makes it unfavourable, and the concentration of the interstitial hydrogen will remain low. An estimate of the fractional concentration of dissolved H atoms in ruthenium is 10^{-9} relative to the gas, at 1 bar and room temperature; this is according to a lattice gas model with all H atoms in the lower-energy octahedral sites. The low solubility is confirmed by experimental data[11] and other computational studies.[28]

The elementary hops for hydrogen diffusion in the Ru lattice, as well as their effective frequencies and energy barriers are shown in Fig. 3. We obtain for the diffusion prefactors the values $D_{0\perp} = 1.44 \times 10^{-6}$ m^2 s^{-1} and $D_{0\parallel} = 1.70 \times 10^{-7}$ m^2 s^{-1}. The corresponding activation energies are $Q_\perp = 0.80$ eV and $Q_\parallel = 0.69$ eV. Experimental values for hydrogen diffusion in ruthenium are lacking in the literature. However, our results are of comparable magnitude to those reported in *ab initio* studies for H diffusion in α-titanium.[29]

Hydrogen diffusion in the near-surface region

A hydrogen atom in the first subsurface layer may diffuse in a number of directions, indicated by the arrows and labels in Fig. 4: (1) within the subsurface layer, to an adjacent octahedral site (sideways); (2) to a deeper octahedral site (downwards); (3) to the surface (upwards). While the presence of hydrogen or tin (hydrides) on the metal surface may alter the energies, barriers,

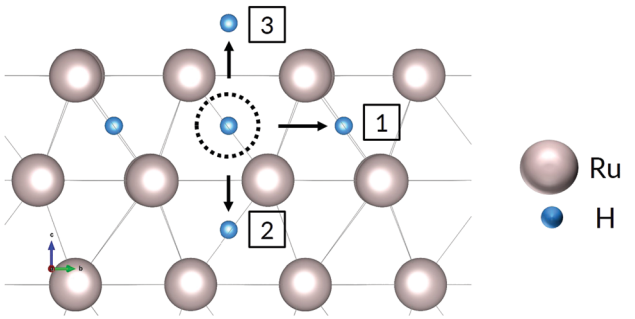

Fig. 4 Diffusion paths for H atom in first Ru subsurface interstitial site. The sideways arrow shows one of six (6) possible diffusion paths within the same subsurface layer.

and precise mechanics of the jumps, the picture remains essentially unchanged with respect to the possible migration paths. It should be noted that the tetrahedral sites may also be occupied by the interstitial atoms. However, due to the high energy of formation compared to the more stable octahedral sites, we have chosen to neglect the effect of tetrahedral site occupancy on the processes discussed.

We distinguish three main example surface/subsurface scenarios, and model the hydrogen atom jumps. As illustrated in Fig. 5, these configurations are: (a) with the surface clear of hydrogen; (b) with adsorbed hydrogen; (c) and with adsorbed hydrogen and tin. For each case, the diffusion paths for the hydrogen atom in the subsurface are calculated using the Climbing Image Nudged Elastic Band (CINEB) algorithm. The results are presented in detail below, and summarised in Table 1.

(a) Clean ruthenium surface. The subsurface octahedral void is surrounded by six (6) identical voids in the same layer. The hydrogen atom may diffuse to any of these sites, across the same short distance and through identical transition states, if the surface and surrounding voids are not occupied. This diffusion step, with the Ru surface clean of adsorbates, is illustrated by Fig. 6a; the energy barrier is 0.73 eV. Diffusion into the deeper bulk interstitial (downwards) is shown in Fig. 6b. There is only one site directly accessible, and the barrier for this jump is slightly higher, at 0.78 eV. The H atom can also diffuse to the surface fcc site, as shown in Fig. 6c, over the much lower barrier of 0.17 eV.

(b) With hydrogen adsorbed. The subsurface diffusion paths were simulated with 100% hydrogen coverage of the Ru(0001) surface, 1 H atom per surface Ru atom. Compared to the situation with a surface devoid of adsorbates, the interstitial hydrogen atom faces a similar energy barrier for diffusion within the layer, 0.78 eV, while the jump into a deeper octahedral void is over a reduced barrier of 0.48 eV. However, the path to the surface is blocked due to the occupation of the fcc site. Only upon diffusion or desorption of the adsorbed hydrogen can the subsurface hydrogen access the vacated site. An example of this multi-step diffusion to the surface is shown in Fig. 7. As an alternative, the atom in the metal may recombine with the atom on the surface to form an H_2 molecule and desorb from the surface (Fig. 8), but this entails overcoming a 1.20 eV energy barrier, much larger than the barrier for a solitary atom moving from subsurface to surface. Furthermore, with an otherwise clean surface and with all fcc sites occupied, this associative desorption ends in a state higher in energy than the starting point. In other words, the adsorbed atom is so low in energy (−0.63 eV relative to a free H_2 molecule) that it compensates the energy cost of the interstitial atom (+0.34 eV).

Table 1 Energy barriers to hydrogen diffusion from subsurface octahedral site. ΔE, the difference in energy between the initial and end states, is given in brackets. The values in italics show associative desorption (AD) (see Fig. 8)

	Energy barrier (ΔE) [eV]		
	Clean surface	H adsorbed	H & Sn adsorbed
Sideways	0.73 (+0.00)	0.78 (+0.00)	0.95 (+0.12)
Downwards	0.78 (+0.02)	0.48 (−0.17)	0.56 (+0.06)
Upwards	0.17 (−0.93)	—	—
Upwards (AD)	—	1.20 (+0.13)	1.89 (+0.03)

(c) With hydrogen and tin adsorbed. The energy barriers for the same three diffusion paths are changed further by the presence of tin on the surface. At this concentration – one Sn atom per 16 Ru and 15 H – the energy barrier to deeper penetration into the metal is 0.56 eV. The sideways diffusion becomes more difficult, however, with its barrier now at 0.95 eV. This may explained by the H atom interacting with the Sn atom on the surface. Most importantly, the associative desorption of hydrogen from the interstitial and surface sites faces a barrier of 1.89 eV. A direct comparison to the case with a clean Ru(0001) surface shows a starkly-changed energy landscape: the barrier to sideways diffusion within the near-surface layer is nearly twice as high as the barrier to deeper penetration, and the barrier to exit is even higher when no fcc site on the surface is free.

4 Discussion

We have put forward a model of the diffusion of an H atom in the Ru lattice, focusing on the paths available to an atom in the

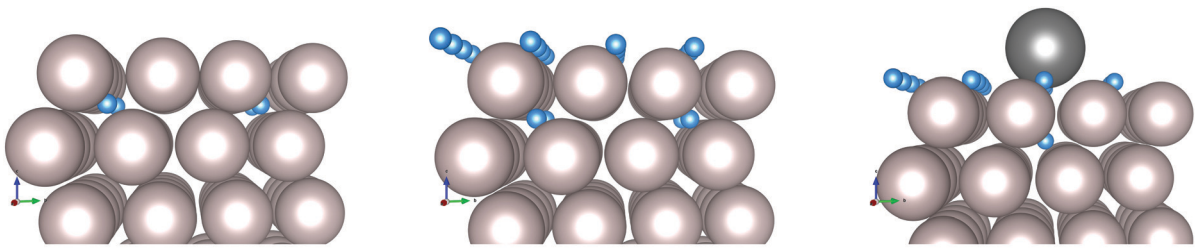

Fig. 5 H in subsurface interstitial sites under a (a) clean Ru surface; (b) Ru surface with H adsorbed; and (c) Ru surface with Sn and H adsorbed.

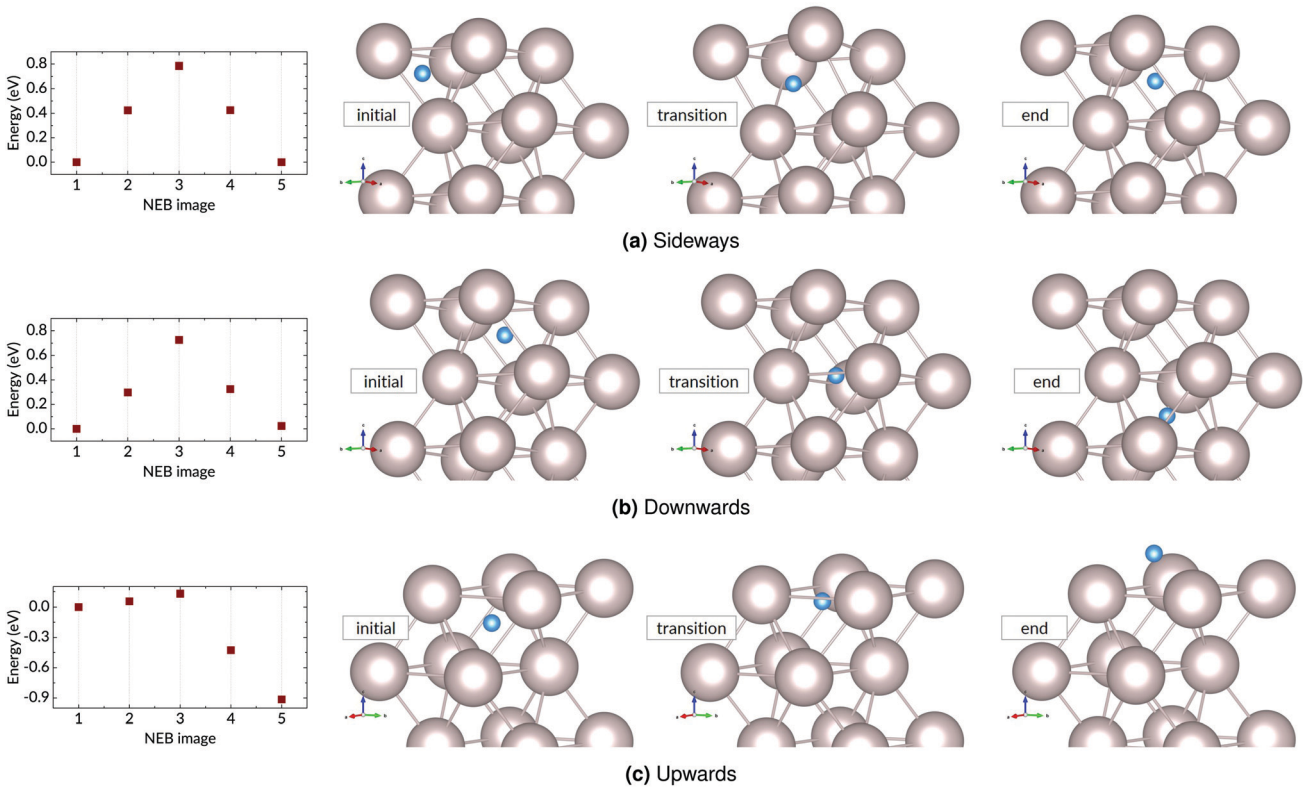

Fig. 6 Diffusion paths for H atom in subsurface under a clean ruthenium surface. The results of 5-image NEB calculations, as well as initial, transition, and end states are shown for: (a) sideways diffusion within the layer; (b) downwards into a deeper layer; and (c) upwards to the surface.

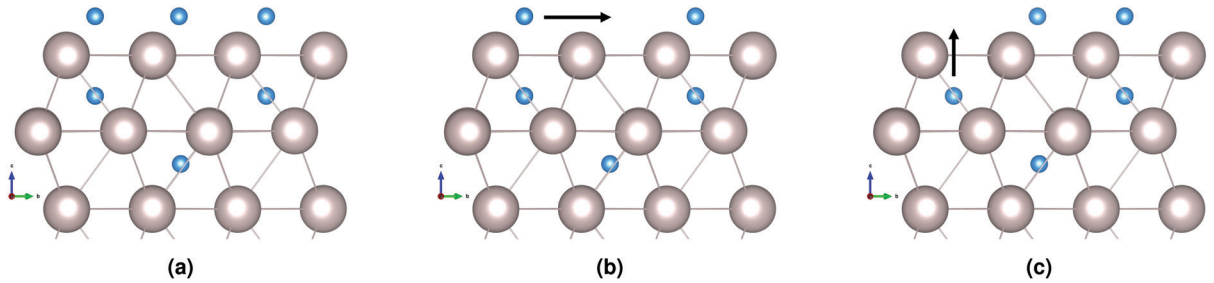

Fig. 7 Multi-step diffusion from subsurface to surface. (a) Surface sites are all occupied, (b) adjacent site is vacated and adatom can move to it, (c) surface site is free and atom in interstitial site can move to the surface.

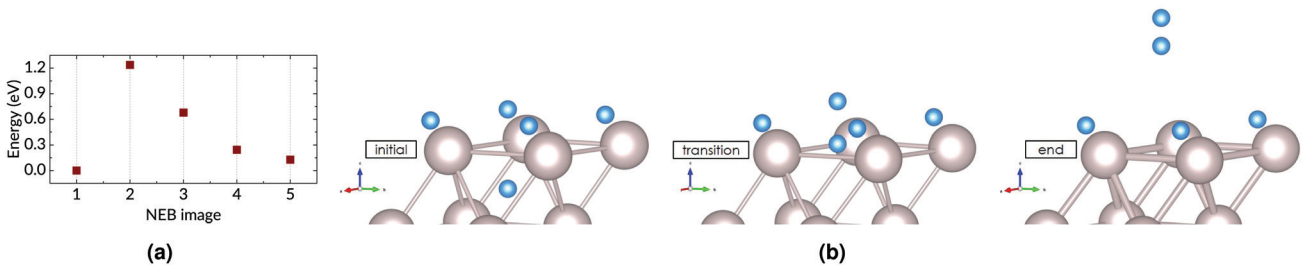

Fig. 8 (a) The result of a 5-image NEB calculation; and (b) the initial, transition, and end states for associative desorption of hydrogen from subsurface octahedral and surface fcc sites, with 1 H atom adsorbed per surface Ru atom.

near-surface region. Each of the diffusion steps presented in the preceding section faces its own peculiar combination of barriers and probabilities.

The sideways jump faces different barriers for the clear and occupied states of the surface, though the 0.05 eV difference is quite slight. In other words, the conditions for the atom

diffusing within the layer are essentially unchanged by the presence of hydrogen on the surface. However, when Sn is present, this sideways diffusion changes: the barrier and ΔE are higher. This is explained by the proximity of the Sn atom, as the change in energy is a result of the change in position relative to the Sn atom and its immediate neighbours.

Moving deeper into the bulk is a relatively simple one-step process, from one octahedral site to another, over a barrier of 0.48–0.78 eV. There is only one destination site, directly below the initial site. If this site happens to be occupied, this migration becomes impossible. This site is unlikely to be occupied, however, owing to the +0.34 eV formation energy and the consequent low solubility of H in Ru. It is notable that this downwards hop results in a lowering of energy (−0.17 eV) relative to the subsurface site when the surface is covered with hydrogen, tilting the situation in favour of deeper migration.

The interstitial atom can also move to the fcc site on the surface, over a barrier that is only 0.17 eV when the surface is clear of adsorbates. This is a much lower barrier than the others faced by the diffusing atom, much more likely to be scaled. Moreover, due to the lower total energy of the adsorbed state, this is an exothermic process, with the end state 0.93 eV lower in energy than the starting point in the interstitial site. However, this escape is contingent on the fcc site being unoccupied. In the case of an occupied surface site, the subsurface-to-surface transition becomes a multi-step process which must involve the vacation of a surface site for the H atom, due to diffusion or recombination. When there is a steady supply of H atoms and molecules to the surface (as is the case when the multi-layer mirror is exposed to H plasma), the interstitial H atom is also in competition for surface sites with this H supply. Each of these conditions reduces the probability of escape, and increases the likelihood of deeper penetration.

A similar site-blocking effect has been proposed to explain the retarded dissociation of YH_3 under a Ru film.[17] Soroka *et al.* observed that the unavailability of surface sites prevented the escape of hydrogen. By raising the temperature of the sample above the desorption temperature, the hydrogen atoms released from the YH_3 layer were able to diffuse to the surface much more rapidly, allowing the decomposition of the yttrium trihydride to proceed. In this instance, only hydrogen adatoms were present. In other studies, the presence of other species, such as carbon or chemically active gases, will reinforce the blocking effect not just by occupying the surface but also by impeding the recombination and desorption of hydrogen.[15]

In the case of a ruthenium thin film exposed to plasma containing a large fraction of atomic hydrogen, the availability of surface sites is limited. Hydrogen readily adsorbs on the ruthenium surface. This means that any hydrogen which ends up within the ruthenium faces an obstacle to escape. The "injection" of hydrogen into the subsurface is caused by the presence of tin, which lowers the penetration barrier.[13] The diffusion coefficients we have calculated indicate that hydrogen diffusion within the ruthenium proceeds at a rate similar to that of hydrogen in other metals, and poses no great obstacle. Tin on the surface also affects surface diffusion of hydrogen, *i.e.* it may reduce the rate at which sites are freed.[13] Thus the likelihood of diffusion to the interface and subsequent blistering is greatly increased when the concentration of hydrogen in the subsurface is significantly raised. In this way, the surface site blocking effect of hydrogen and tin plays a key role in the blistering of the ruthenium film. To be perfectly accurate in answering our initial question: the hydrogen which enters the ruthenium thin film does eventually leave; it simply ends up in the blisters at the opposite face.

5 Conclusion

In this article we have presented the case for the influence of surface saturation on hydrogen diffusion to the interface between a ruthenium thin film and its substrate, *via* an examination of the diffusion paths available to a hydrogen atom in the interstitial site just beneath a Ru(0001) surface. By performing transition state calculations of the key hydrogen migrations, we have shown a clear effect of surface occupancy on the energy barriers to diffusion of a hydrogen atom in the near-surface interstices. Our results indicate that the blocking of access to the surface results in increased likelihood of diffusion deeper into the metal lattice. In conjunction with the reduced energy barrier to subsurface penetration in the presence of tin, this effect leads to accumulation of hydrogen in the metal and interface, and subsequent blistering of the ruthenium thin film. This indicates that modifying and controlling the surface coverage may be an effective method of controlling the amount of hydrogen retained in the metal and underlying layers.

Author contributions statement

S. T. and T. M. conceived the study, C. O. performed the calculations. All authors analysed the results and reviewed the manuscript.

Conflicts of interest

There are no conflicts of interest to declare.

Acknowledgements

This research was carried out under project number T16010a in the framework of the Partnership Program of the Materials innovation institute M2i (www.m2i.nl) and the Technology Foundation TTW (www.stw.nl), which is part of the Netherlands Organization for Scientific Research (www.nwo.nl).

References

1 C. Bruneau and P. H. Dixneuf, *Ruthenium in Catalysis*, Springer International Publishing, 2014, vol. 48.
2 A. G. Knapton, *Platinum Met. Rev.*, 1977, **21**, 44–50.
3 N. A. Al-Mufachi, N. V. Rees and R. Steinberger-Wilkens, *Renewable Sustainable Energy Rev.*, 2015, **47**, 540–551.
4 B. Sakintuna, F. Lamari-Darkrim and M. Hirscher, *Int. J. Hydrogen Energy*, 2007, **32**, 1121–1140.

5 T. Hübert, L. Boon-Brett, G. Black and U. Banach, *Sens. Actuators, B*, 2011, **157**, 329–352.
6 Y. Ueda, J. Coenen, G. De Temmerman, R. Doerner, J. Linke, V. Philipps and E. Tsitrone, *Fusion Eng. Des.*, 2014, **89**, 901–906.
7 Y. B. He, A. Goriachko, C. Korte, A. Farkas, G. Mellau, P. Dudin, L. Gregoratti, A. Barinov, M. Kiskinova, A. Stierle, N. Kasper, S. Bajt and H. Over, *J. Phys. Chem. C*, 2007, **111**, 10988–10992.
8 S. Bajt, H. N. Chapman, N. Nguyen, J. B. Alameda, J. C. Robinson, M. E. Malinowski, E. Gullikson, A. Aquila, C. Tarrio and S. Grantham, *Proc. SPIE*, 2003, **5037**, 236–248.
9 A. S. Kuznetsov, R. W. E. van de Kruijs, M. A. Gleeson, K. Schmid and F. Bijkerk, *J. Surf. Invest.: X-Ray, Synchrotron Neutron Tech.*, 2010, **4**, 563–566.
10 A. S. Kuznetsov, M. A. Gleeson and F. Bijkerk, *J. Appl. Phys.*, 2014, **115**, 173510.
11 R. B. McLellan and W. A. Oates, *Acta Metall.*, 1973, **21**, 181–185.
12 P. Feulner and D. Menzel, *Surf. Sci.*, 1985, **154**, 465–488.
13 C. Onwudinanti, I. Tranca, T. Morgan and S. Tao, *Nanomaterials*, 2019, **9**, 1–18.
14 A. I. Livshits, M. E. Notkin and A. A. Samartsev, *J. Nucl. Mater.*, 1990, **170**, 79–94.
15 Y. Ueda, T. Shimada and M. Nishikawa, *Nucl. Fusion*, 2004, **44**, 62–67.
16 S. Ogura, M. Okada and K. Fukutani, *J. Phys. Chem. C*, 2013, **117**, 9366–9371.
17 O. Soroka, J. M. Sturm, R. W. van de Kruijs, C. J. Lee and F. Bijkerk, *Appl. Surf. Sci.*, 2018, **455**, 70–74.
18 G. Kresse and J. Hafner, *Phys. Rev. B: Condens. Matter Mater. Phys.*, 1994, **49**, 14251–14269.
19 G. Kresse and J. Furthmüller, *Comput. Mater. Sci.*, 1996, **6**, 15–50.
20 D. Joubert, *Phys. Rev. B: Condens. Matter Mater. Phys.*, 1999, **59**, 1758–1775.
21 J. D. Perdew, K. Burke and M. Ernzerhof, *Phys. Rev. Lett.*, 1996, **77**, 3865–3868.
22 G. Henkelman, B. P. Uberuaga and H. Jónsson, *J. Chem. Phys.*, 2000, **113**, 9901–9904.
23 H. King, *CRC Handbook of Chemistry and Physics*, CRC Press, 2012, pp. 15–18.
24 K. K. Irikura, *J. Phys. Chem. Ref. Data*, 2007, **36**, 389–397.
25 S. Ishioka and M. Koiwa, *Philos. Mag. A*, 1985, **52**, 267–277.
26 G. H. Vineyard, *J. Phys. Chem. Solids*, 1957, **3**, 121–127.
27 I. M. Ciobica, A. W. Kleyn and R. A. Van Santen, *J. Phys. Chem. B*, 2003, **107**, 164–172.
28 I. Del Rosal, L. Truflandier, R. Poteau and I. C. Gerber, *J. Phys. Chem. C*, 2011, **115**, 2169–2178.
29 Y. Lu and P. Zhang, *J. Appl. Phys.*, 2013, **113**, 193502.